Similarity in Fog and Rainfall Intermittency

M. Räsänen[1] [ID]**, M. Chung[2], M. Katurji[3]** [ID]**, P. Pellikka[1,4], J. Rinne[5]** [ID]**, and G. G. Katul[6]** [ID]

[1]Institute for Atmospheric and Earth System Research, University of Helsinki, Finland, [2]Department of Civil and Environmental Engineering, University of California, Berkeley, CA, USA, [3]Centre for Atmospheric Research, University of Canterbury, Christchurch, New Zealand, [4]Earth Change Observation Laboratory, Department of Geosciences and Geography, University of Helsinki, Helsinki, Finland, [5]Department of Physical Geography and Ecosystem Science, Lund University, Lund, Sweden, [6]Nicholas School of the Environment, Duke University, Durham, NC, USA

Abstract Intermittent fog occurrences supply significant amounts of moisture to plants in the form of fog drip onto the soil surface thereby prompting interest in their statistical behavior at multiple timescales. A comparison of rainfall and fog measurements collected at an inland tropical cloud forest in Kenya and a coastal rangeland in Northern California is presented to explore whether fog occurrences have similar intermittency characteristics as rainfall. The results confirm that both rainfall and fog show approximate power law relations for distributions of dry period and event size consistent with predictions from self-organized criticality. Moreover, the spectral exponents of the on-off time series of the fog and rainfall exhibited an approximate $f^{-0.8}$ over a broad range of frequencies f, which is remarkably close to scaling exponents across sites experiencing different rainfall generation mechanisms. These results suggest that fog intermittency shares some properties of critical behavior documented in numerous rainfall studies.

Plain Language Summary Beyond rainfall, intermittent fog occurrence provides water subsidy that is needed for sustaining transpiration and photosynthesis in forests. To study the connections between fog formation and rainfall, a comparison of rainfall and fog occurrence statistics is carried out at two sites: a Kenyan inland cloud forest and a coastal forest in Northern California. For durations exceeding 1 day, rainfall and fog event sizes and dry periods appear similar. Due to these similarities, intermittency in fog occurrences may abide by general laws describing critical phenomenon.

1. Introduction

Fog plays an important role for several microclimates such as western continental margins, montane cloud forests, and several deserts (Bruijnzeel et al., 2005; Garreaud et al., 2008; Kaseke et al., 2017). Frequent fog occurrence leads to cool and humid environment with reduced transpiration rates and wet soils thereby supporting water demands for photosynthesis. Fog season may coincide with dry season and contribute to the water balance or increase ecosystem drought resilience (Chung et al., 2017). Unsurprisingly, connections between fog and rainfall statistics are now drawing research interest in hydrological, ecological, and climate-related sciences. The most elementary connection is similarity in their on-off switching properties at multiple timescales and this connection frames the scope of this letter.

The switching between rain/no rain or fog/no fog describes the on/off phases of the precipitation and fog time series. Because the off phases are ordered (or quiescent) but the on phases are disordered and variable in time, such phase transitions resemble systems near critical states. Moreover, there are certain mean meteorological variables, viewed here as control parameters, that favor switching from ordered to disordered or vice versa. Because these meteorological variables fluctuate in space and time during a single large-scale fog or rainfall event due to turbulence, the two phases can spatially coexist. Thus, the boundary delineating these two phases need not be discontinuous at the fog or rainfall event scale. Such phase transitions are referred to as second-order phase transitions and the region delineating the two phases (ordered versus disordered) is known as critical state. Critical states are said to be on the edge of chaos because certain symmetries are broken during the phase transition (Pruessner, 2012). A prototypical model for such phase transition is self-organized critically (SOC), which has been studied extensively in the context of rainfall but not fog. Rainfall event size (continuous measurement of rainfall), event duration and dry period distributions often follow a power law scaling (Peters & Christensen, 2006; Peters et al., 2010). These observations are necessary but not

sufficient conditions for SOC to hold. Although recent analysis did not confirm universality for critical exponents of rainfall as may be expected in other phase transitions between ordered (no rain, the off phases) and disordered (rainy or foggy, the on phases) states (Deluca et al., 2016), the SOC paradigm remains a pragmatic model for rainfall description (Pruessner, 2012). A similar analysis of fog events has yet to be conducted so as to understand possible connections between fog and rainfall occurrences.

The analysis here is conducted using high-frequency measurements of fog deposition and rainfall at an inland tropical montane cloud forest in Kenya and at a coastal Northern Californian chaparral rangeland. The objectives are twofold: (i) Is SOC an acceptable descriptor of rainfall intermittency at the two measurement sites as has been reported across numerous sites? (ii) Does fog intermittency resemble an SOC process? If so, does it inherit some of its SOC features from rainfall? This study focuses mainly on the on-off features of rainfall and fog, not amounts. Hence, a suitable approach to utilize is the so-called telegraphic approximation (TA) of the time series. The TA is simply a binary representation that transforms the series into *on* (or unity) and *off* (or null) values. The TA is not concerned with amplitude variability within the on phases. Because the work here seeks to explore similarity in switching between on-off and off-on phases in rainfall and fog, the focus is on spectra, zero-crossing density statistics over time intervals, and dry period durations. Where necessary, event size is also considered.

One pragmatic benefit of documenting analogies to SOC (or to other corollary mechanisms) is the potential use of established theoretical results linking spectral scaling exponents describing the switching memory and durations of ordered states. Another benefit is that certain exponents may signify deeper links between fog and sporadic randomness examined in the context of rainfall (Rigby & Porporato, 2010). One universal mechanism describing intermittency associated with switching between periodicity and pure randomness is the Pomeau-Manneville Type III intermittency (PM3I). Other pragmatic benefits are numerous and include (i) stochastic simulation of occurrences of fog durations, clustering properties, and realistic switching between fog/no-fog phases; (ii) documenting connections between exponents (e.g., spectra of TA and duration of off phases) that can then be used to check (or test) whether detailed physical models are able to reproduce such relations among exponents; and (iii) allowing new physics to be discovered about fog and second-order phase transitions. Moreover, the resulting exponents determined and discussed here can offer clues about the dynamics governing rainfall and fog at particular range of temporal scales (or changes in the aforementioned dynamics with changing scales).

2. Methods

2.1. Measurements

The inland measurement site is in an opening within Vuria forest (3°24′50″S, 38°17′29″E) of the Taita hills located 200 km from the Kenyan coast (Figure S1 in the supporting information). The Taita hills has biannual rainy seasons with short rains from October to December and long rains from late March to June. Seasonality and amount of rainfall vary over short distances depending on the altitude and the aspect of the slope whereas the interannual variation of rainfall has strong spatial coherence (Nicholson, 2017). At the Taita hills, higher elevations receive more rain because of orographic rainfall pattern, while the northwestern slope in the rain-shadow receives less precipitation compared with the southeastern slopes (Pellikka et al., 2013). Due to the high-altitude location, the site has frequently advection fog but radiation fog events are also possible. The measurement site is surrounded by degraded elfin forest or upper montane cloud forest at 2,176 m above the sea level described elsewhere (Stam et al., 2017). Meteorological variables and fog deposition time series were measured from October 2013 to February 2016. The measured variables include mean wind speed and direction, air temperature, relative humidity, soil moisture at 10 cm depth, rainfall, and fog deposition rates. All variables were sampled every minute and recorded every hour. The fog collector was a typical fog net with a double layer of Raschel-type netting (Schemenauer & Cereceda, 1994). The fog net surface area was 1 m² and the gutter area was 1.15 m by 0.12 m (= 0.138 m²). The deposited fog water was measured using a tipping bucket rain gauge protected from rainfall. The fog net was facing northwest (320°) and southeast (140°) and had a metal plate roofing covering it from rainfall.

The coastal Northern Californian site is located at Spring Valley Ridge, on the San Francisco Peninsula, at 329 m above the sea level. The fog collector was a Juvik-type radial collector above a chaparral rangeland. Details of the experimental setup and the spatial analysis of fog at this watershed are presented elsewhere (Chung et al., 2017) and are not repeated here. The fog deposition and rainfall were measured from June 2014 to September 2016. The fog deposition was not measured during winter months at this site, but it is expected

that non-rainfall-related fog events are minimal relative to rainfall during the winter months. The rainfall was continuously measured except during one 40-day-long gap in November 2015. Hereafter, the Kenyan and California sites are labeled as inland and coastal, respectively.

To analyze fog and rainfall time series independently, fog deposition during rainfall was excluded from the analysis. In addition, fog events that had rainfall events of 1.0 mm or larger 2 hr before the fog event were excluded from the fog record. Both rainfall and fog events were defined as a continuous nonzero measurement of rainfall and fog. Isolated 0.2-mm/h events were also removed from both time series as this threshold sets the detection limit of the tipping bucket.

2.2. Analysis Methods

The analysis used to quantify on-off statistics in fog deposition and rainfall time series over differing timescales has been used in turbulence research (Sreenivasan et al., 1983; Sreenivasan & Bershadskii, 2006), including studies on temperature fluctuations in convection, velocity, and scalar concentration fluctuations within canopies, and atmospheric surface layer turbulence over several surface roughness regimes and density stratification (Cava & Katul, 2009; Cava et al., 2012; Poggi & Katul, 2009; Sreenivasan et al., 2004).

The same method has been successfully applied to the study of rainfall intermittency (Molini et al., 2009) and root-zone soil moisture dynamics (Ghannam et al., 2016). In these methods, the TA is used to explore the on-off switching of fog deposition and rainfall (Sreenivasan & Bershadskii, 2006) as well as any memory in the switching.

To illustrate, consider a time series $s(t)$ representing either fog deposition or rainfall amounts. The $TA(s)$ is defined as

$$TA(s(t)) = \frac{1}{2}\left[\frac{s(t) - s^*}{|s(t) - s^*|} + 1\right],$$

(1)

where s^* is a threshold to be exceeded. Here $s^* = 0$ for both rainfall and fog occurrence. Because $TA(s(t))$ is a binary series composed of either 1 or 0 in time, it only preserves the on-off or off-on switching in $s(t)$ but contains no information about magnitude variation.

When the spectra of $s(t)$ and its $TA(s)$ time series exhibit power laws of the form $E_{ns}(f) \sim f^{-n}$ and $E_{TA}(f) \sim f^{-m}$, there exists an empirical relation between the spectral exponents given by

$$m = \frac{n+1}{2},$$

(2)

where n is the spectral exponent of $s(t)$ and m is the spectral exponent of $TA(s)$. This expression appears to hold across a broad range of stochastic processes including $1/f$ noise, which is a scale-free process. It approximately holds for the well-studied PM3I, where $m \approx 1.6$ (determined empirically by us through simulations) and $n = 3/2$. A PM3I is paradigmatic of a behavior intermediate between periodicity and pure randomness, often labeled as sporadic randomness (Pomeau & Manneville, 1980; Rigby & Porporato, 2010). The normalized time series used in the determination of the spectra is given by

$$s_n(t) = \frac{s(t) - \overline{s(t)}}{\sigma_s},$$

(3)

where $\overline{s(t)}$ is the mean and σ_s is the root-mean-square value of series $s(t)$. All the spectra were estimated using the Welch-averaged modified periodogram method (Welch, 1967). The window length was set to a quarter of the time series length.

The cluster exponent quantifies the scaling of the local standard deviation of the density of the zero crossings (Sreenivasan & Bershadskii, 2006). The running density of zero crossings is $\psi(T) = N(T)/T$ in a time interval T. The fluctuations of this quantity are $\delta\psi(T) = \psi(T) - \langle\psi(T)\rangle$, and the local standard deviation is $\langle\delta\psi(T)^2\rangle^{1/2}$ presumed to decay as

$$\langle\delta\psi(T)^2\rangle^{1/2} \propto T^{-\alpha},$$

(4)

where α is the cluster exponent. For a white noise process, the cluster exponent is $\alpha = 0.5$ and this value indicates no tendency of clustering of zero crossings in time (or space). Exponents with $\alpha < 0.5$ indicate increasing clustering tendency, at least when compared to white noise.
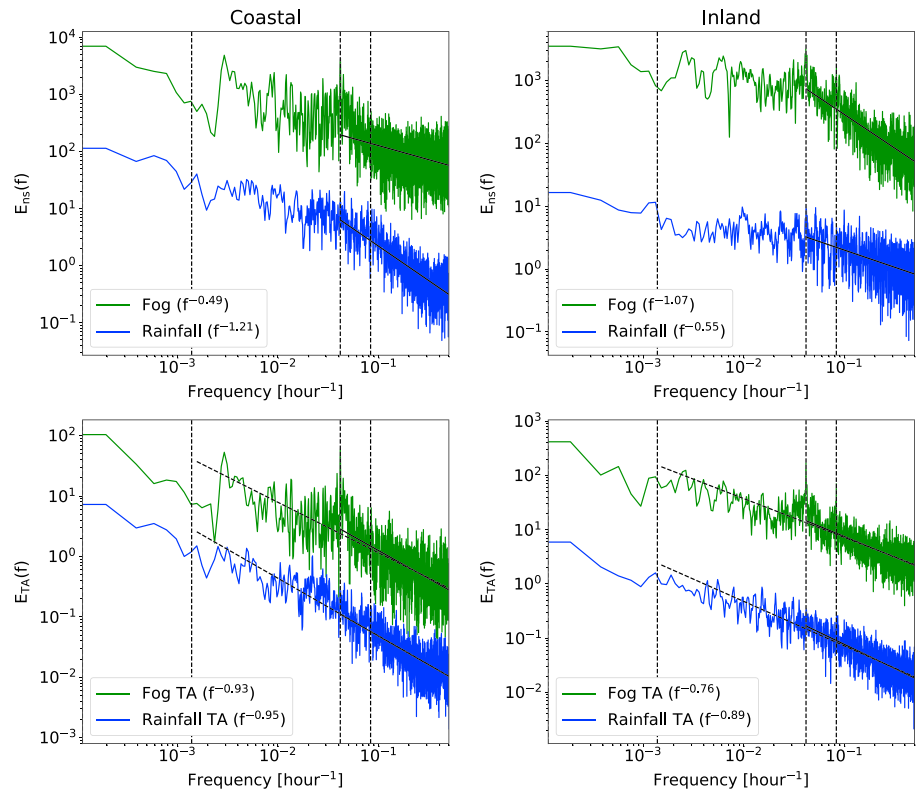
Figure 1. Normalized spectrum of fog and rainfall time series and their corresponding telegraphic approximation (TA) spectra. The linear fit is up to 1 day, and dashed fit line extends to 1 month. The dashed vertical lines show frequencies corresponding to 12-hr, 24-hr, and 1-month timescales for clarity. The fog spectra were shifted along the *y* axis to permit comparisons.

SOC predicts a probability density function (PDF) of the duration of dry periods (T_d) and event sizes (M) that exhibit power laws of the form

$$p(T_d) \propto T_d^{-\tau_d}, \quad p(M) \propto M^{-\tau_s}. \tag{5}$$

The dry period PDF is defined by the distribution of periods when $TA(s(t)) = 0$. Commonly used least squares fitting can produce inaccurate estimates of power law exponents (Clauset et al., 2009). Here power laws were fitted using a maximum-likelihood method, which identifies the portion of the distribution that follows a power law (Alstott et al., 2014).

3. Results

Before discussing intermittency in fog and rainfall at the two sites, few general remarks about these time series are highlighted. There were foggy days during some 23% of the time period at the inland site, while fog occurred only about 6% of the days at the coastal site. Hence, The frequency of fog events differ appreciably between sites. Topography at the coastal site influenced fog occurrence frequency and much of the fog can be considered advective. Moreover, rainfall and fog were almost out of phase with each other. At the inland site, the highest fog deposition amounts coincided with rainfall maximums at monthly timescales (Figures S2 and S3). Interestingly, fog occurrence at the coastal site here appeared similar to a seasonal rain forest in southwest China, where fog drip was mainly observed during the dry season and its amount was estimated to be 5% of annual rainfall (Liu et al., 2004). At the inland site, the total rainfall during the measurement period was 2388 mm and the final total fog deposition was 965 mm/m^2 after excluding the rainfall effects. In total, there were 418 fog events from which 71 events were excluded from the analysis due to rainfall occurrences before the fog event. At the coastal site, the total rainfall during the measurement period was 1,501 mm and there were 65 fog events adding up to 86 mm/m^2 of total fog deposition.

At the coastal site, suppression of evapotranspiration and its concomitant water savings is much more significant (Chung et al., 2017). At the inland site, at least one fog event occurred every month on record but most
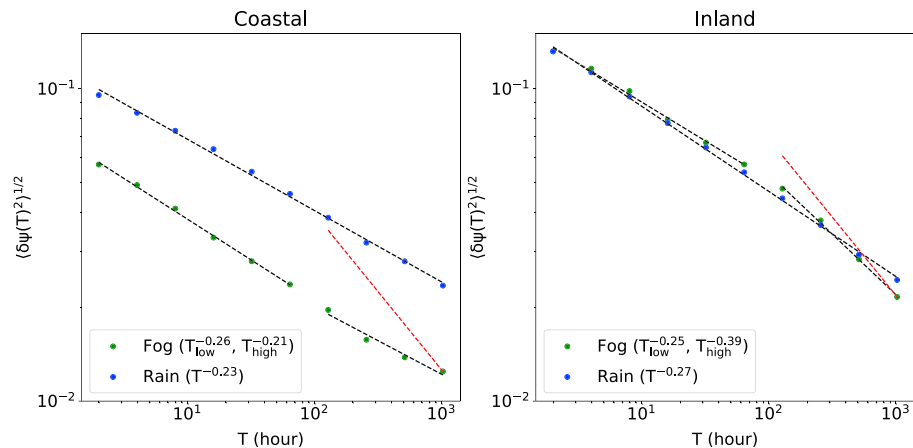
Figure 2. Standard deviation of the running density fluctuations against scale T for the fog and the rainfall time series. The dashed red line indicates clustering for a white noise process.

fog deposition amounts were between November and April. Due to the bimodal rainfall distribution and frequent fog occurrence, the forest at the top of Vuria is not experiencing sustained drought periods. The average diurnal fog deposition had two maxima at 7 a.m. and 8 p.m. whereas the diurnal rainfall had a maximum at 4 p.m. (Figure S4). The coastal site did not have diurnal peaks in diurnal fog deposition (Figure S5).

3.1. Spectrum of Rainfall and Fog

The rainfall and fog deposition spectra exhibit power law decay at subdaily periods (Figure 1). The fog deposition at both sites had a mild-bump at 24 hr, whereas the inland site exhibited an additional bump at 12 hr. While small in magnitude, this bump could be an indication of nighttime-forming fog events that then evaporated during the morning hours at the inland site. The data available here do not permit us to explore this conjecture further. The coastal fog spectrum is flattening at high frequency, which is like due inadequate sampling of fog events. This flattening is absent in the TA spectrum. Typical rainfall spectra exhibit approximate power law scaling regimes at the frontal (roughly f^{-1}) and convective (roughly $f^{-0.5}$) timescales (Molini et al., 2009). The measurements here were recorded at one hour interval and perhaps not sufficiently short to resolve the shortest timescales associated with such storms. In the transition region (1 month to 3 days), the rainfall and fog spectra appear similar (Figure 1). With regard to the TA spectra ($E_{TA}(f)$) of the rainfall and fog series, a number of features can be pointed out: (i) Similar scaling laws were evident in the two series ($f^{-0.93}$ and $f^{-0.95}$ at the coastal site and $f^{-0.76}$ and $f^{-0.89}$ at the inland site for fog and rainfall, respectively), and (ii) the scaling laws in both TA series extended over a broad range of timescales — from hourly to monthly scales. The actual rainfall and fog series exhibited scaling laws only at the subdaily timescales. This finding is suggestive of remarkable similarity in the on-off and off-on switching for fog and rainfall across a much broader range of timescales when compared to the spectra of the actual time series. The TA exponents here (for both rainfall and fog) are close to a previously reported value of 0.84 derived from long-term precipitation data at five sites experiencing vastly different rainfall formation patterns and confirms that this exponent appears to be robust to microclimatic variation (Molini et al., 2009).

The rainfall spectral exponent and TA exponent at less than 1-day period were $n = 0.55$ and $m = 0.89$ for inland and $n = 1.21$ and $m = 0.95$ for the coastal site. The analysis of inland site here confirm that the spectrum of the full rainfall series decays slower than its TA counterpart (i.e., more determinism in the TA than in the actual rainfall series), consistent with prior studies (Molini et al., 2009).

For inland site, the full fog time series spectra decayed faster than its TA counterpart, whereas for the coastal site the opposite was true. The difference between spectral exponent of TA and the predicted exponent from equation (2) were −0.28 and 0.19 for fog and 0.12 and −0.16 for rainfall for inland and coastal site, respectively. Because equation (2) was derived for fractional Brownian motion and similar stochastic processes exhibiting extensive power laws, the agreement reported here is suggestive of a broader connection between spectra and their TA counterpart for rainfall and fog. The TA spectral decay are similar for all time series but the full series spectrum can decay with rates lower or higher than their TA counterpart. Hence, the switching between
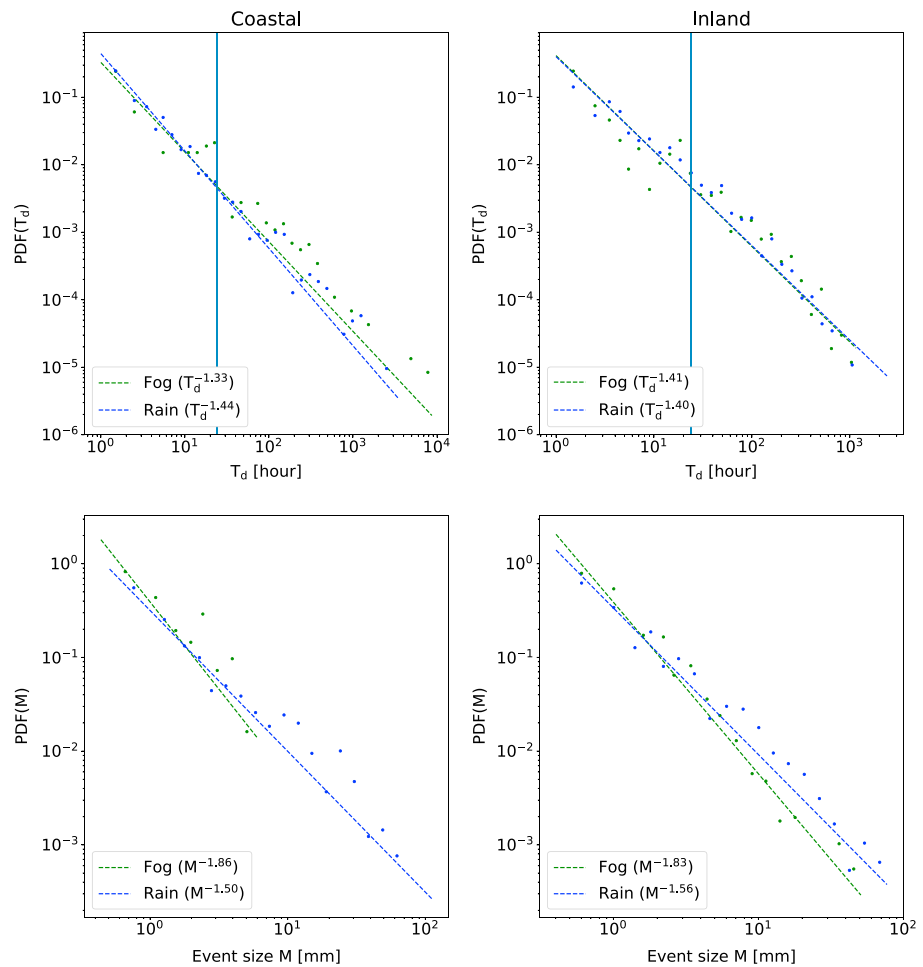
Figure 3. The probability density functions (PDFs) of the duration of dry periods and the event sizes for rainfall and fog deposition measurements. The blue vertical line denotes 1-day period. Note that the rainfall and fog deposition size PDFs do not have the same units because the fog deposition amount has units of millimeters per 1 m^2 of fog net.

ordered (off) and disordered (on) states may be sufficiently robust thereby inviting analogies to well-studied phenomenon such as SOC exhibiting similar scaling laws.

3.2. Cluster Exponent

The cluster exponents for rainfall have an approximate power law relation, whereas the fog clustering exponents exhibit a regime change at around 5- to 10-day period (Figure 2). The rainfall cluster exponents were 0.23 and 0.27 for coastal and inland sites. These values are lower than the nearly constant $\alpha = 0.33$ reported for rainfall sampled across differing microclimatic regimes (Molini et al., 2009). The difference between these two aforementioned exponents may be related to orographic effects present at both measurement sites here but absent in the data sets featured in the aforementioned study (Molini et al., 2009).

At the inland site, the two scaling regimes in the cluster exponent emerge in the fog time series with values of $\alpha_{low} = 0.25$ ($T < 5$ days) and $\alpha_{high} = 0.39$ (T > 5 days), whereas the coastal site has values of $\alpha_{low} = 0.26$ and $\alpha_{high} = 0.21$ (Figure 2). Due to the lower number of fog events and larger interannual variability of fog frequency at the coastal site, the clustering exponent estimation might not be as robust as the inland site. At the inland site, the fog deposition events have a tendency to cluster together more at shorter than 5-day intervals. The two scaling regimes in the fog time series clustering may also be an artifact of the fog sampling method. The fog collector might not collect fog amounts during light fog events that would lead to separation of one fog event into two events. To test for this effect, the TA of inland fog time series was modified by combining fog events that are less than 2 hr apart into one event. For this modified fog time series, the cluster exponents determined by repeating the same analysis were $\alpha_{low} = 0.31$ and $\alpha_{high} = 0.36$.

The fact that the exponents remain distinct suggests that scaling difference cannot be entirely explained by artifacts in fog collection.

3.3. The Dry Period and Event Size PDF

The dry period and event size PDF of rainfall and fog deposition at both sites exhibit a power law decay (Figure 3) consistent with the SOC paradigm. The scaling exponents of the dry period PDFs were $\tau_d = 1.33$ and $\tau_d = 1.41$ for fog and $\tau_d = 1.44$ and $\tau_d = 1.40$ for rainfall at the coastal and inland sites, respectively. The scaling exponents for rainfall appear to be surprisingly similar to the one reported for radar measurements of rainfall in Germany (Peters & Christensen, 2006). Similarly, Deluca and Corral (2014) determined an exponent of 1.5 ± 0.05 using 20 tipping bucket rainfall measurements around the Mediterranean coast in Spain. Over 1-day long, dry periods have a tendency to be above the power law fit line for up to around 16 days at the inland site. This deviation from a power law in the dry period PDF has also been reported in previous studies (Deluca & Corral, 2014; Peters & Christensen, 2006). The largest scatter in the fog dry period PDF is at less than 1-day periods. For longer periods, the fog PDF is similar to its rainfall counterpart. This finding is consistent with the observed similarity in the spectra for rainfall and fog at transition regions. The longer dry periods in the fog time series resemble the statistics of the rainfall.

For SOC systems near critical state, there exists a unique relation between the spectral exponent of the TA time series and the exponent of the dry period PDF given by $m = 3 - \tau_d$ derived and confirmed for the avalanches of the classical sandpile model near critical slopes (Jensen, 1998). The estimated TA exponent varied from 1.56 to 1.67 for fog and rainfall. Differences between the measured TA exponent and the predicted one from SOC is large ranging from -0.61 to -0.84. This finding suggests that amplitude intermittency effects in the active (or on phases) appreciably contributed to the relation between m and τ_d. Intermittency corrections were estimated using the squared temporal gradients, and they varied from 0.41 to 0.49 for TA series and 0.54 to 0.86 for full time series. These corrections are similar to previous estimates for rainfall and confirm that neither the full time series nor TA-derived corrections are large enough to account for the large difference between the two m estimates (Molini et al., 2009). The fact that the $m = 3 - \tau_d$ is not fully realized here implies that the SOC and PM3I models cannot fully explain all aspects of the on-off and off-on switching for both fog and rainfall despite the emergence of power laws in many of the statistics evaluated here. That is, amplitude variations within the *on phases* are impacting the relation between m and τ_d. The rainfall event size scaling exponents were 1.50 and 1.56 for coastal and inland sites, respectively. These values are closer to the value reported for the northwestern Mediterranean coast $\tau_s = 1.5 \pm 0.05$ (Deluca & Corral, 2014) than for a global data set $\tau_s = 1.17$ (Peters et al., 2010). The former study employed tipping bucket data, whereas the global data set used an optical measurement technique. The difference in measurement techniques might explain some of the differences in exponents. The tipping bucket measurements can underestimate rainfall amounts under windy conditions whereas the optical measurement technique is optimized for a particular droplet size distribution.

The fog event size scaling exponents were similar ($\tau_s = 1.8$) at both sites. The units of the event sizes between rainfall and fog are different because the fog deposition is measured per 1 m^2 of fog net. At the inland site, there are small deviations from the power law fit in the size PDF around 3.4 and 5.4 mm for fog and rainfall, respectively. The coastal fog size PDF extends less than an order of magnitude and does not allow for robust exponent determination.

4. Discussion, Conclusion, and Future Outlook

The seductiveness of the SOC paradigm is that complex systems (i.e., systems with many interacting parts whose macroscopic dynamics cannot be characterized by a single or limited number of scales) may exhibit universal statistical patterns in the form of power laws. SOC is deemed to be a property of a dynamical system that has a critical point (or phase transition between order and disorder) as its attractor. Because many complex systems near critical points exhibit power law behavior or scale invariance (in space or time or both), these power law exponents may be quasi-universal. SOC allows for the exponents of various statistics to be related to each other when the dynamics of the system self-tune to stay near the attractor or critical point (e.g., $m = 3 - \tau_d$).

Analogies between rainfall and fog deposition based on the SOC paradigm were explored here. The premise here is that ordered states are associated with *no-fog* or *no-rain* periods, whereas disordered states are associated with variable fog and rainfall amounts. The focus here were on the transitions between ordered and

disordered states and not on the amplitude intermittency within the disordered states. The essential ingredients for the aforementioned SOC analogy were based on the fact that the event size, the spectra and their TAs, the clustering exponents, and the dry period PDFs all exhibit approximate power laws in rainfall and in fog time series. The value of the exponents and possible relations among them were analyzed.

One of the main findings is that the TA spectra for both fog and rainfall time series exhibited an extensive power law scaling regime well beyond the timescales of the spectra of the original series with exponents $m \approx 0.76$–0.95. The $m \approx 0.8$ exponent in the TA here agrees well with prior studies on rainfall time series where the dominant generation mechanism differed appreciably across data sets. The SOC relation between the measured exponent of the TA spectra m and the exponent of the dry period PDF τ_d (i.e., $m = 3 - \tau_d$ for SOC) has also been considered. This expression reasonably describes the PM3I process (checked by us via simulations not shown here). In turbulence studies, this deviation from SOC predictions has been attributed to intermittency corrections resulting in $m + \tau_d = 3 - \mu_l$. The computed μ_l from second-order gradients (for the full series and its TA transform) appeared to be insufficient in all cases (i.e., $m + \tau_d + \mu_l < 3$). This finding points to the fact that the switching between active and passive phases is not entirely independent from the amplitude intermittency within the active phases (as is the case in SOC or PM3I).

The fog statistics deviated from their rainfall counterparts at the subdaily timescales where the dry period PDF have larger scatter and fog spectra exhibit mild but noticeable bumps at 12- and 24-hr periods absent in rainfall. Presumably, these differences result in scale separation in the fog clustering patterns at around 5-day period, also absent in rainfall. In fact, no apparent *break* in cluster exponent for rainfall was detected across scales.

Notwithstanding these distortions and breaks, it can be surmised that the TA analysis of the fog time series offers further evidence for some element of critical behavior as in rainfall (at least in its on-off or off-on switching). However, the analogy to SOC (or PM3I) is not entirely complete even within the confines of TA transformations. Satellite observations of rainfall have confirmed that important observables of rainfall are predicted by theory of critical phenomena (Peters & Neelin, 2006). Whether similar success can be juxtaposed to fog remains a subject of future inquiry. The work here offered several tantalizing clues and highlighted several limitations of the SOC paradigm.

References

Alstott, J., Bullmore, E., & Plenz, D. (2014). Powerlaw: A python package for analysis of heavy-tailed distributions. *Plos One*, *9*(1), e85777.

Bruijnzeel, L. A., Eugster, W., & Burkard, R. (2005). Fog as a hydrologic input. In M. G. Anderson, & J. J. McDonnell (Eds.), *Encyclopedia of Hydrological Sciences* (pp. 559–582). Chichester, UK: John Wiley & Sons, Ltd. https://doi.org/10.1002/0470848944.hsa041

Cava, D., & Katul, G. G. (2009). The effects of thermal stratification on clustering properties of canopy turbulence. *Boundary-Layer Meteorology*, *130*(3), 307–325. https://doi.org/10.1007/s10546-008-9342-6

Cava, D., Katul, G. G., Molini, A., & Elefante, C. (2012). The role of surface characteristics on intermittency and zero-crossing properties of atmospheric turbulence. *Journal of Geophysical Research*, *117*, D01104. https://doi.org/10.1029/2011JD016167

Chung, M., Dufour, A., Pluche, R., & Thompson, S. (2017). How much does dry-season fog matter? Quantifying fog contributions to water balance in a coastal California watershed. *Hydrological Processes*, *31*(22), 3948–3961. https://doi.org/10.1002/hyp.11312

Clauset, A., Shalizi, C. R., & Newman, M. E. J. (2009). Power-law distributions in empirical data. *SIAM Review*, *51*(4), 661–703. https://doi.org/10.1137/070710111

Deluca, A., & Corral, Á. (2014). Scale invariant events and dry spells for medium-resolution local rain data. *Nonlinear Processes in Geophysics*, *21*, 555–567. https://doi.org/10.5194/npg-21-555-2014

Deluca, A., Puig, P., & Corral, Á. (2016). Testing universality in critical exponents: The case of rainfall. *Physical Review E*, *93*(4). https://doi.org/10.1103/PhysRevE.93.042301

Garreaud, R., Barichivich, J., Christie, D. A., & Maldonado, A. (2008). Interannual variability of the coastal fog at Fray Jorge relict forests in semiarid Chile. *Journal of Geophysical Research*, *113*, G04011. https://doi.org/10.1029/2008JG000709

Ghannam, K., Nakai, T., Paschalis, A., Oishi, C. A., Kotani, A., Igarashi, Y., et al. (2016). Persistence and memory timescales in root-zone soil moisture dynamics. *Water Resources Research*, *52*, 1427–1445. https://doi.org/10.1002/2015WR017983

Jensen, H. J. (1998). *Self-Organized Criticality: Emergent Complex Behavior in Physical and Biological Systems*. Cambridge: Cambridge University Press.

Kaseke, K. F., Wang, L., & Seely, M. K. (2017). Nonrainfall water origins and formation mechanisms. *Science Advances*, *3*(3), e1603131.

Liu, W., Meng, F.-R., Zhang, Y., Liu, Y., & Li, H. (2004). Water input from fog drip in the tropical seasonal rain forest of Xishuangbanna, South-West China. *Journal of Tropical Ecology*, *20*(05), 517–524. https://doi.org/10.1017/S0266467404001890

Molini, A., Katul, G. G., & Porporato, A. (2009). Revisiting rainfall clustering and intermittency across different climatic regimes. *Water Resources Research*, *45*, W11403. https://doi.org/10.1029/2008WR007352

Nicholson, S. E. (2017). Climate and climatic variability of rainfall over eastern Africa. *Reviews of Geophysics*, *55*, 590–635. https://doi.org/10.1002/2016RG000544

Pellikka, P., Clark, B., Gosa, A., Himberg, N., Hurskainen, P., Maeda, E., et al. (2013). Chapter 13—Agricultural expansion and its consequences in the Taita Hills, Kenya. *Developments in Earth Surface Processes*, *16*, 165–179. https://doi.org/10.1016/B978-0-444-59559-1.00013-X

Peters, O., & Christensen, K. (2006). Rain viewed as relaxational events. *Journal of Hydrology*, *328*(1-2), 46–55. https://doi.org/10.1016/j.jhydrol.2005.11.045

Peters, O., Deluca, A., Corral, A., Neelin, J. D., & Holloway, C. E. (2010). Universality of rain event size distributions. *Journal of Statistical Mechanics: Theory and Experiment*, *2010*(11), P11030. https://doi.org/10.1088/1742-5468/2010/11/P11030

Peters, O., & Neelin, J. D. (2006). Critical phenomena in atmospheric precipitation. *Nature Physics*, *2*(6), 393–396. https://doi.org/10.1038/nphys314

Poggi, D., & Katul, G. (2009). Flume experiments on intermittency and zero-crossing properties of canopy turbulence. *Physics of Fluids*, *21*(6), 065103. https://doi.org/10.1063/1.3140032

Pomeau, Y., & Manneville, P. (1980). Intermittent transition to turbulence in dissipative dynamical systems. *Communications in Mathematical Physics*, *74*(2), 189–197.

Pruessner, G. (2012). *Self-Organised Criticality: Theory, Models and Characterisation*. New York: Cambridge University Press.

Rigby, J. R., & Porporato, A. (2010). Precipitation, dynamical intermittency, and sporadic randomness. *Advances in Water Resources*, *33*(8), 923–932. https://doi.org/10.1016/j.advwatres.2010.04.008

Schemenauer, R. S., & Cereceda, P. (1994). A proposed standard fog collector for use in high-elevation regions. *Journal of Applied Meteorology*, *33*(11), 1313–1322.

Sreenivasan, K. R., & Bershadskii, A. (2006). Clustering properties in turbulent signals. *Journal of Statistical Physics*, *125*(5-6), 1141–1153. https://doi.org/10.1007/s10955-006-9112-0

Sreenivasan, K. R., Bershadskii, A., & Niemela, J. J. (2004). Multiscale SOC in turbulent convection. *Physica A: Statistical Mechanics and its Applications*, *340*(4), 574–579. https://doi.org/10.1016/j.physa.2004.05.008

Sreenivasan, K. R., Prabhu, A., & Narasimha, R. (1983). Zero-crossings in turbulent signals. *Journal of Fluid Mechanics*, *137*, 251–272. https://doi.org/10.1017/S0022112083002396

Stam, Å., Enroth, J., Malombe, I., Pellikka, P., & Rikkinen, J. (2017). Experimental transplants reveal strong environmental effects on the growth of non-vascular epiphytes in Afromontane forests. *Biotropica*, *49*, 862–870. https://doi.org/10.1111/btp.12472

Welch, P. (1967). The use of fast fourier transform for the estimation of power spectra: A method based on time averaging over short, modified periodograms. *IEEE Transactions on Audio and Electroacoustics*, *15*(2), 70–73. https://doi.org/10.1109/TAU.1967.1161901